Zeitschrift: Schweizerische mineralogische und petrographische Mitteilungen =

Bulletin suisse de minéralogie et pétrographie

Band: 82 (2002)

Heft: 2: Diagenesis and Low-Grade Metamorphism

Artikel: Correlation of fluid inclusion temperatures with illite "crystallinity" data

and clay mineral chemistry in sedimentary rocks from the external part

of the Central Alps

Autor: Mullis, Josef / Rahn, Meinert K. / Schwer, Peter

DOI: https://doi.org/10.5169/seals-62368

Nutzungsbedingungen

Die ETH-Bibliothek ist die Anbieterin der digitalisierten Zeitschriften auf E-Periodica. Sie besitzt keine Urheberrechte an den Zeitschriften und ist nicht verantwortlich für deren Inhalte. Die Rechte liegen in der Regel bei den Herausgebern beziehungsweise den externen Rechteinhabern. Das Veröffentlichen von Bildern in Print- und Online-Publikationen sowie auf Social Media-Kanälen oder Webseiten ist nur mit vorheriger Genehmigung der Rechteinhaber erlaubt. Mehr erfahren

Conditions d'utilisation

L'ETH Library est le fournisseur des revues numérisées. Elle ne détient aucun droit d'auteur sur les revues et n'est pas responsable de leur contenu. En règle générale, les droits sont détenus par les éditeurs ou les détenteurs de droits externes. La reproduction d'images dans des publications imprimées ou en ligne ainsi que sur des canaux de médias sociaux ou des sites web n'est autorisée qu'avec l'accord préalable des détenteurs des droits. En savoir plus

Terms of use

The ETH Library is the provider of the digitised journals. It does not own any copyrights to the journals and is not responsible for their content. The rights usually lie with the publishers or the external rights holders. Publishing images in print and online publications, as well as on social media channels or websites, is only permitted with the prior consent of the rights holders. Find out more

Download PDF: 30.11.2025

ETH-Bibliothek Zürich, E-Periodica, https://www.e-periodica.ch

Correlation of fluid inclusion temperatures with illite "crystallinity" data and clay mineral chemistry in sedimentary rocks from the external part of the Central Alps

by Josef Mullis¹, Meinert K. Rahn^{2,*}, Peter Schwer³, Christian de Capitani¹, Willem B. Stern¹ and Martin Frey¹ (deceased)

Abstract

A data set of 71 samples from 42 localities within the external part of the Central Alps is used to compare illite "crystallinity" (IC) and deconvolution fitted peak parameters with fluid inclusion homogenization temperatures from fibre quartz. Fluid inclusions are filled with methane-bearing fluid and were trapped within a temperature range of 200–270 °C. For the majority of localities, carbonate-rich samples show lower IC values than the clay-rich samples, due to retardation of illite crystal growth by early cementation and conservation of the primary, detrital clay fraction. A small number of localities, however, indicate the opposite trend; these are characterized by high ratios of dolomite versus clay minerals in the carbonate-rich sample. Based on chemical and mineralogical data for the clay fraction, we conclude that the presence of dolomite in these samples implies early diagenetic precipitation of salts in semi-arid to arid climates, triggering the formation of early Na-rich smectite.

All deconvoluted phases (chlorite, smectitic phase, illitic-muscovitic phase) show simple trends in their full-width-at-half-maximum and peak position versus fluid inclusion homogenization temperature. A major control on illite "crystallinity" is the amount of the smectitic phase, which varies from 35 to 82%. However, even if the amount of smectitic phase is considered as an independent variable besides temperature, the correlation with illite "crystallinity" is weak and underlines the only semiquantitative character of illite "crystallinity" as a thermal indicator. The clay fraction compositional evolution shows that anchizonal "illites" contain more K, but less Na than their diagenetic counterparts. For K an external source, probably K-feldspar, has to be assumed. From the data set, a temperature of 240 ± 15 °C is derived for the boundary between diagenesis and anchizone (IC = $0.42 \, \Delta^{\circ} 2\theta$), which is distinctly higher than so far assumed in the literature.

Keywords: Central Alps, fluid inclusion temperatures, illite crystallinity, deconvolution, diagenesis, anchizone, dolomite.

Introduction

Illite "crystallinity" has been widely used to determine the metamorphic grade in subgreenschist facies pelitic rocks (FREY, 1987). The term "crystallinity" refers to the observed width at half height of the 10 Å reflection (KÜBLER, 1967). However, this width at half height is based not only on the status of an illitic structure, i.e. the X-ray scattering domain size of a K-deficient mica structure, but also on the presence of other miner-

al phases, such as smectites, the stacking order between illitic and smectitic layers (e.g. Lanson and Champion, 1991), and the reaction progress towards equilibrium (Merriman and Peacor, 1999). Therefore, the crystal growth process is not simply the result of a rearrangement of the structure of a single phase with temperature, but depends also on other factors, such as the initial detrital substratum, the supply of cations by migrating fluids, the structural evolution of the host rock, and the kinetics of crystal growth (Frey,

¹ Mineralogisch-Petrographisches Institut, Universität Basel, Bernoullistrasse 30, CH-4056 Basel, Switzerland. <josef.mullis@unibas.ch>

² Institut für Mineralogie Petrologie und Geochemie, Albert-Ludwigs-Universität, Albertstrasse 23b, D-79104 Freiburg, Germany.

^{*} Present address: HSK, CH-5232 Villigen, Switzerland.

³ Eichrainweg 6b, CH-6410 Goldau.

1987). The term "crystallinity" is used here as representing the sum of all factors, including the increase in compositional homogeneity, the decrease in interlayered swelling components, and the advancing perfection of the illite crystal structure (JABOYEDOFF et al., 2001). While a large number of studies describe the transition from smectite to illite qualitatively (e.g. ROBINSON and SANTANA DE ZAMORA, 1999; BAULUZ et al., 2000), little systematic work has been devoted to the various limiting conditions of evolution.

This study from the external part of the Central Alps presents a correlation between illite "crystallinity" values and fluid inclusion homogenization temperatures, the latter of which are taken as a close approximation of the maximum temperatures reached during Neoalpine burial. Rock samples were collected from localities with fluid inclusion homogenization temperatures between 200 and 270 °C. A detailed evaluation of the illite "crystallinity" as an indicator of incipient metamorphism was done by application of a deconvolution fitting procedure to the X-ray diffraction pattern.

Geology and sampling strategy

The Helvetic belt represents a stack of sedimentary nappes that evolved during the Mesozoic and early Tertiary at the northern border of the Tethys Ocean, between the Eurasian and Apulian plates. The northward movement of the African plate, passively pushing the Apulian microplate, led to a closure of the Tethys beginning in mid Cretaceous, and to a continent-continent collision in the Eocene. This terminated sedimentation in the Helvetic belt and started nappe formation from S to N. Burial under tectonic units of more southern origin is documented today by the presence of Penninic and Austroapline klippen on top of the Helvetic nappe stack. This burial led to a diagenetic to lowermost greenschist facies overprint increasing in grade from N to S.

The metamorphic gradient within the Helvetic belt has been documented along several profiles in the Central Alps (e.g. FREY et al., 1980; BREITSCHMID, 1982; RAHN et al., 1995), with the help of extended data sets on illite "crystallinity" (e.g. WANG et al., 1996; FERREIRO-MÄHLMANN,

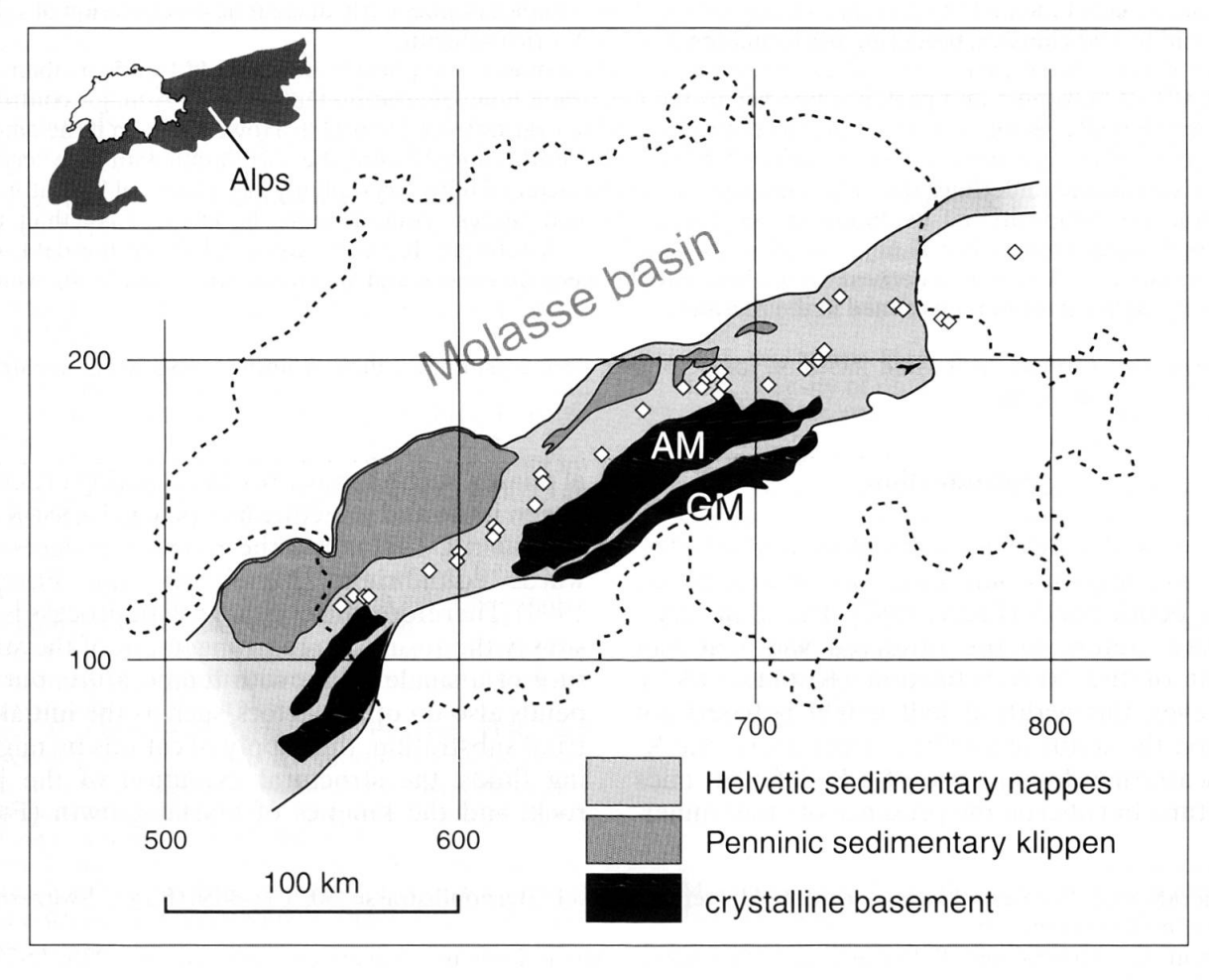


Fig. 1 Sample localities in the northern parts of the Central Alps. For various localities, multiple samples of varying carbonate contents were taken. Coordinates correspond to Swiss map grid (1 unit = 1 km). AM—Aar massif, GM—Gotthard massif.

1995, 1996), vitrinite reflectance (ERDELBROCK, 1994; FERREIRO-MÄHLMANN, 1994, 1995, 1996), and fluid inclusion homogenization temperatures (MULLIS, 1979, 1987). In addition to the classic division into a diagenetic, anchizonal and epizonal belt, the combined applications resulted in a correlation of different methods, and led to the definition of several subzones within the diagenetic and anchizonal realm (e.g. FERREIRO-MÄHLMANN, 1996). In addition to this zonation, other regional divisions were proposed, in particular three fluid zones (MULLIS, 1979, 1987), based on characteristic fluid inclusion compositions: Higher hydrocarbon-rich fluids dominate in the north, methane-dominated fluids are characteristic for the intermediate zone, and methanedepleted water-rich fluids are found in the south. All samples for this study were taken from the methane zone, with maximum homogenization temperatures between 200 and 270 °C, as measured within syn-kinematically grown fissure quartz (Fig. 1). Fluid inclusion homogenization temperatures are interpreted as approximate formation temperatures on the basis of the following arguments: (a) structural field evidences: the boundary between the methane and the water zone crosscuts internal folds in the Helvetic nappes and is itself cut by younger thrust faults (e.g. Breitschmid, 1982, Mullis et al., 1994); (b) fluid inclusion petrography: fluid inclusions that formed during prograde conditions display stretching or decrepitation features, whereas undeformed fluid inclusions were formed during and after peak temperature conditions (MULLIS, 1997); and (c) measured homogenization temperatures of the earliest non-stretched or non-decrepitated fluid inclusions always yield the highest values in all investigated Alpine fissures (MULLIS, 1979, 1987). The samples chosen for this study all fulfill strict requirements for inclusion formation close to peak conditions of diagenesis or metamorphism. For all samples the geologic context suggests similar P-T paths, thus excludes large differences between fluid inclusion and illite "crystallinity" data due to the fact that the former method represents a snapshot of physical conditions during the moment of fluid entrapment, while the latter is thought to be the result of reaction progress and crystal growth during the entire diagenetic/metamorphic evolution.

At several localities, two or three samples were taken within a distance of a few metres, but with large variation in carbonate content. Such a set typically includes a sample of minimum of carbonate component (shale, sample number A, Table 1), a marl of intermediate carbonate content (B), and a carbonate-rich marl to marly lime-

stone (C). With increasing content in carbonate phases (calcite, dolomite), samples commonly lose their schistose appearance.

The data presented originate from 71 samples taken at 42 different localities within the methane zone (MULLIS, 1987) of the Central Alps. Sample localities are displayed in Fig. 1 and listed in Table 1.

Principles and methods

Rock samples were milled and the bulk rock powder measured by XRD for semiquantitative phase determination. After removal of the carbonate phases and application of Atterberg separation techniques, the fraction <2 μ m of the samples was sedimented on glass slides with a constant amount of 5 mgcm⁻². These clay-fraction slides were used for both ED-XRF and XRD analysis. The chemical composition of the <2 μ m fraction was measured by ED-XRF using the instrumental equipment and procedure described by STERN et al. (1991). All clay fraction samples were analyzed using a Siemens D-500 diffractometer (Cu-K α radiation, 40 kV, 30 mA, automatic divergence slits, secondary graphite monochromator).

XRD measurement procedures for deconvolution and classic illite "crystallinity" determination are described in detail in STERN et al. (1991), and satisfy the requirements proposed by KISCH (1991). The full-width-at-half-maximum (FWHM) of the unresolved 10Å complex was determined online after background subtraction, and measured values were corrected against an internal standard (epizonal rock chip). This was followed by mathematical deconvolution fitting of overlapping peaks. The range of diffraction angles chosen for deconvolution varied between 4–11 °2θ (three peaks) in cases where, after background subtraction, no zero level was reached between the first chlorite reflection and the illite-smectite peak complex, and 7–11 °2θ (two peaks) in those cases, where the first chlorite peak was completely separated from the illite-smectite complex.

The deconvolution procedure depends on a number of important conditions and assumptions, which have a distinct influence on the results. Without detailed discussion, which is found elsewhere (e.g. Lanson and Champion, 1991; Lanson and Besson, 1992; Lanson and Velde, 1992; Stern et al., 1991), the most important assumptions applied in this study are as follows:

(1) All X-ray reflections derived from single mineral phases are assumed to be symmetric (Lanson and Champion, 1991). The variation in tailing of the illite peak during diagenesis and within the anchizone (as defined by KÜBLER et al.,

Central Alps. FWHM = full width at half maximum, IC = illite "crystallinity" as defined by KUBLER et al. (1979). IC values are given with three digits, though the Table 1 XRD raw file and deconvolution fitted data (CuK_a radiation) and XRF compositional data for samples from the "methane zone" in northern parts of the significance of the third digit may be questionable.

| Sample no. locality | locality | Swiss map coordinates Thom | oordinates | $T_{ m hom}$ | FWHMFWHM $(\Delta^{\circ}2\theta)$ $(\Delta^{\circ}2\theta)$ | FWHM $(\Delta^{\circ}2\theta)$ | illitic-m | illitic-muscovitic phase | phase | sme | smectitic phase | ıse | | chlorite | | COU | XRF chemical composition | n n |
|---------------------|--------------------------|----------------------------|------------|--------------|--|--------------------------------|--------------------------------|--------------------------|---------------|--------------------------------|-----------------|------------------|--------------------------------|----------------|------------------|----------------------|--------------------------|------------|
| | | horizontal vertical | vertical | (°C) | air-dried g | air-dried glycolated (=IC) | FWHM $(\Delta^{\circ}2\theta)$ | d-value (Å) p | XRD peak area | FWHM $(\Delta^{\circ}2\theta)$ | d-value (Å) | XRD peak area | FWHM $(\Delta^{\circ}2\theta)$ | d-value (Å) | XRD peak area | K ₂ O wt% | Na ₂ O wt% | MgO wt% |
| Mu-003 | Rengglipass | 627.560 | 162.040 | 223 | 1.926 | 0.974 | 0.516 | 10.097 | 62 | 1.429 | 10.974 | 303 | 0.507 | 14.129 | 59 | 3.51 | 0.52 | 5.12 |
| Mu-003A | 3 | | | 223 | 1.767 | 1.118 | 0.430 | 10.040 | 94 | 1.803 | 11.111 | 510 | 0.384 | 14.129 | 33 | 4.35 | 0.65 | 2.23 |
| Mu-003C | | | | 223 | 1.994 | 1.048 | 0.637 | 9.983 | 158 | 1.575 | 11.182 | 307 | 0.412 | 14.129 | 37 | 4.23 | 0.88 | 2.06 |
| Mu-010A1 | Bundstock S | 625.045 | 151.380 | 267 | 0.362 | 0.393 | 0.251 | 10.009 | 154 | 0.518 | 10.267 | 203 | 0.311 | 14.175 | 52 | 6.44 | 0.32 | 2.41 |
| Mu-010B | | | | 267 | 0.299 | 0.341 | 0.214 | 10.015 | 100 | 0.496 | 10.250 | 135 | 0.290 | 14.216 | 55 | 90.9 | 0.11 | 3.23 |
| Mu-024-1 | First | 647.250 | 168.250 | 247 | 0.616 | 0.526 | 0.346 | 10.040 | 140 | 0.702 | 10.394 | 203 | 0.249 | 14.129 | 19 | 4.10 | 0.24 | 1.00 |
| Mu-024-1A | | | | 247 | 0.735 | 0.711 | 0.473 | 9.983 | 165 | 1.102 | 10.517 | 243 | 0.387 | 14.129 | 29 | 5.90 | 0.55 | 1.06 |
| Mu-031 | Isleten | 687.920 | 196.630 | 210 | 0.658 | 0.532 | 0.396 | 10.056 | 64 | 1.015 | 10.588 | 138 | 0.288 | 14.177 | 57 | 3.96 | 0.13 | 7.06 |
| Mu-035 | Attinghausen | 689.300 | 192.220 | 262 | 0.397 | 0.378 | 0.271 | 10.000 | 112 | 0.818 | 10.401 | 186 | 0.385 | 14.195 | 44 | 5.88 | 0.44 | 2.95 |
| Mu-035A |) | | | 262 | 0.544 | 0.418 | 0.292 | 10.002 | 126 | 0.817 | 10.430 | 292 | 0.368 | 14.158 | 4 | 7.38 | 0.13 | 2.80 |
| Mu-035B | | | | 262 | 0.418 | 0.378 | 0.246 | 9.955 | 103 | 0.680 | 10.278 | 212 | 0.344 | 14.116 | 34 | 6.44 | 0.50 | 3.07 |
| Mu-058A | Choex | 563.900 | 120.800 | 242 | 0.391 | 0.398 | 0.262 | 696.6 | 112 | 0.589 | 10.257 | 188 | 0.224 | 14.127 | 46 | 7.10 | 0.10 | 3.16 |
| Mu-058B | | | | 242 | 0.424 | 0.489 | 0.339 | 10.014 | 129 | 0.662 | 10.369 | 168 | 0.284 | 14.197 | 34 | 7.55 | 0.00 | 3.05 |
| Mu-059A1 | Massongez | 564.400 | 121.350 | 237 | 0.475 | 0.463 | 0.303 | 876.6 | 87 | 899.0 | 10.308 | 138 | 0.319 | 14.207 | 43 | 7.15 | 0.03 | 5.01 |
| Mu-059B1 |) | | | 237 | 0.397 | 0.391 | 0.262 | 066.6 | 104 | 0.674 | 10.318 | 171 | 0.259 | 14.170 | 54 | 5.99 | 0.23 | 2.89 |
| Mu-061A1 | Tour de Duin | 567.730 | 121.420 | 244 | 0.440 | 0.398 | 0.271 | 9.985 | 173 | 0.656 | 10.286 | 295 | 0.253 | 14.148 | 75 | 6.41 | 0.05 | 3.33 |
| Mu-061B | | | | 244 | 0.380 | 0.437 | 0.275 | 666.6 | 112 | 929.0 | 10.318 | 194 | 0.321 | 14.184 | 9 | 5.46 | 0.26 | 2.86 |
| Mu-062A | Les Monts | 569.700 | 120.900 | 241 | 0.429 | 0.419 | 0.293 | 666.6 | 134 | 0.762 | 10.359 | 500 | 0.360 | 14.177 | 80 | 5.54 | 0.32 | 2.73 |
| Mu-062B1 | | | | 241 | 0.440 | 0.408 | 0.293 | 9.995 | 228 | 0.694 | 10.335 | 343 | 0.343 | 14.143 | 107 | 6.01 | 0.25 | 2.50 |
| Mu-068-1 | Sanetschpass | 590.000 | 129.860 | 228 | 0.889 | 0.764 | 0.526 | 10.097 | 528 | 1.018 | 10.580 | 620 | 0.261 | 14.129 | 98 | 99.5 | 0.75 | 2.24 |
| Mu-071A | Tschingelloch | 611.750 | 143.800 | 216 | 0.593 | 0.564 | 0.404 | 10.073 | 31 | 1.007 | 10.511 | 20 | 0.291 | 14.275 | 9 | 2.31 | 0.13 | 1.55 |
| Mu-072 | Engstligengrat | 612.000 | 142.900 | 202 | 0.824 | 809.0 | 0.370 | 10.040 | 29 | 1.016 | 10.517 | 16 | 0.357 | 14.129 | 4 | 2.37 | 0.15 | 2.56 |
| Mu-072A | | | | 202 | 0.984 | 0.764 | 0.471 | 10.021 | 53 | 1.331 | 10.576 | 137 | 0.393 | 14.110 | 18 | 4.50 | 0.43 | 3.64 |
| Mu-072B | | | | 202 | 0.708 | 0.721 | 0.434 | 10.011 | 70 | 1.345 | 10.475 | 134 | 0.298 | 14.152 | 24 | 3.73 | 0.42 | 3.38 |
| Mu-073A | Tierhörnli | 611.720 | 141.250 | 230 | 0.846 | 0.777 | 0.571 | 9.983 | 117 | 1.180 | 10.644 | 131 | 0.327 | 14.129 | 22 | 4.36 | 0.72 | 4.50 |
| Mu-074A | Betlis | 729.450 | 222.000 | 197 | 0.852 | 0.596 | 0.414 | 10.004 | 82 | 0.927 | 10.473 | 145 | 0.574 | 14.156 | 35 | 5.62 | 0.00 | 3.80 |
| Mu-074B | | | | 197 | 0.709 | 0.517 | 0.346 | 9.962 | 55 | 906.0 | 10.401 | 105 | 0.422 | 14.078 | 25 | 4.82 | 0.20 | 3.40 |
| Mu-076 | Strahlrüfi | 747.860 | 218.080 | 223 | 1.053 | 629.0 | 0.456 | 10.064 | 148 | 1.169 | 10.683 | 389 | 0.332 | 14.171 | 09 | 80.9 | 0.21 | 2.36 |
| Mu-076-4 | | | | 223 | 1.110 | 0.650 | 0.417 | 10.078 | 117 | 1.135 | 10.649 | 309 | 0.330 | 14.186 | 85 | 4.13 | 60.0 | 3.37 |
| Mu-077 | Palvris | 749.950 | 217.730 | 236 | 1.321 | 0.893 | 0.491 | 10.084 | 169 | 1.387 | 10.777 | 654 | 0.350 | 14.113 | 89 | 4.06 | 0.74 | 1.70 |
| Mu-077A | | | | 236 | 0.873 | 0.654 | 0.417 | 10.095 | 78 | 1.453 | 10.680 | 190 | 0.313 | 14.209 | 45 | 4.02 | 0.31 | 5.54 |
| Mu-081 | Fontanella | 788.320 | 236.120 | 203 | 1.399 | 0.684 | 0.502 | 10.097 | 144 | 1.292 | 10.773 | 487 | 1.257 | 14.017 | . 62 | 4.46 | 0.25 | 1.30 |
| Mu-202A1 | Ijes Fürggli | 763.770 | 214.020 | 227 | 1.139 | 0.848 | 0.508 | 9.981 | 93 | 1.592 | 10.598 | 239 | 1.516 | 13.683 | 40 | 4.37 | 0.40 | 2.54 |
| Mu-203A | Ijes Fürggli SW | 763.830 | 213.770 | 238 | 0.592 | 0.705 | 0.413 | 9.983 | 103 | 1.208 | 10.517 | 257 | 0.636 | 14.129 | 32 | 5.65 | 0.36 | 2.72 |
| Mu-204A | Barthümeljoch SW 765.880 | SW 765.880 | 213.380 | 226 | 0.643 | 0.529 | 0.377 | 9.983 | 159 | 1.071 | 10.394 | 293 | 0.414 | 14.129 | 28 | 6.36 | 0.00 | 2.46 |
| JAG. 204C | | | | 300 | 0360 | 0 224 | 3900 | 0.067 | 30 | 0090 | 10 202 | 3.4 | 0.240 | 11 107 | 0 | 221 | 0.30 | 117 |

| , | - | - |
|---|---|---|
| | + | ز |
| | 5 | = |
| | 0 | 5 |
| | e | 5 |
| , | | ٥ |
| | | |
| | | |
| 1 | - | 4 |
| | | |
| , | _ | 2 |
| | - | ₹ |
| 1 | - | ะ |
| | | |

| 11 Grat-Attinghauses 11 Val d'Illiez 12 Linthal 13 Rawilpass 14 Lac de Tseuzier 15 Bockialp 16 Klausenpass W 17 Labria 17 Schwarzrüfi 18 Kleintal-Isenthal 19 Grosstal-Isenthal 11 Isenthal 12 Bannalp 13 Betschwanden 14 Haslen 16 Haslen 17 Mollis 18 Untere Lattreien 18 Glütsch 18 Bretternhörnli 19 Glütsch | horizontal vertical n 687.350 189.000 559.700 118.160 717.750 196.800 599.240 135.750 599.090 132.980 661.800 183.400 704.430 192.110 750.970 216.880 748.650 218.840 | (°C) | | | | | | | | | | | | - | - | |
|--|--|------|----------------------|-------|--------------|---------|-------------|---------------------------|---------|-----------|---------------------------|---------|------------|------|------|------|
| 1. Grat-Attinghausen 1. Val d'Illiez 1. Linthal 1. Linthal Rawilpass Lac de Tseuzier Bockialp Klausenpass W Labria Schwarzrüfi Kleintal-Isenthal B Grosstal-Isenthal 1 Isenthal 1 Isenthal 1 Isenthal 1 Isenthal 2 A Kleintal E 3 Bannalp 4 Haslen 1 Mollis 1 Untere Lattreien 1 Glütsch 1 Grasstal-Isenthal | | | air-dried glycolated | | FWHM d-v | d-value | XRD | FWHM | d-value | XRD | FWHM | d-value | XRD | K,O | Na,O | MgO |
| 1.1 Grat-Attinghausen 1.1 Val d'Illiez 1.2 Linthal Rawilpass Lac de Tseuzier Bockialp Klausenpass W Labria Schwarzrüfi Kleintal-Isenthal I Grosstal-Isenthal I Isenthal I Isenthal I Isenthal I Betschwanden Haslen Haslen I Mollis I Untere Lattreien Glütsch Bretternhörnli | | 264 | (=IC) | | (√20) (√20) | (Å) pea | peak area (| $(\Delta^{\circ}2\theta)$ | (Å) F | peak area | $(\Delta^{\circ}2\theta)$ | (Å) I | peak area | wt% | wt% | wt% |
| 1. Val d'Illiez 1. Linthal Rawilpass Lac de Tseuzier Bockialp Klausenpass W Labria Schwarzrüfi Kleintal-Isenthal B 1. Grosstal-Isenthal 1. Isenthal 1. Isenthal 1. Isenthal 2. Mkleintal E 3. Bannalp 4. Kleintal E 5. B 6. Bunnalp 7. Haslen 7. Haslen 8. Haslen 8. Haslen 9. Untere Lattreien 1. Glütsch 1. Glütsch 1. Grosstal-Isenthörnli | | | | 0.333 | | 701 | 119 | 0.574 | 10.283 | 169 | 0.305 | 14.143 | 69 | 5.30 | 0.22 | 3.01 |
| 1. Val d'Illiez 1. Linthal Rawilpass Lac de Tseuzier Bockialp Klausenpass W Labria Schwarzrüfi Kleintal-Isenthal B Grosstal-Isenthal 1 Isenthal 1 Isenthal 1 Isenthal 1 Isenthal 2 Grosstal-Isenthal 1 Isenthal 1 Isenthal 2 Grosstal-Isenthal 3 Grosstal-Isenthal 4 Kleintal E 8 Bannalp 1 Betschwanden 1 Mollis 1 Untere Lattreien Glütsch 1 Gritsch | | 264 | 0.352 | 0.363 | 0.233 10.0 | 10.002 | 98 | 0.585 | 10.285 | 127 | 0.324 | 14.175 | 69 | 4.45 | 0.13 | 3.38 |
| Rawilpass Lac de Tseuzier Bockialp Klausenpass W Labria Schwarzrüfi Kleintal-Isenthal B Grosstal-Isenthal I Isenthal I Isenthal B Bannalp B Bannalp I Betschwanden Haslen Haslen I Mollis I Untere Lattreien Glütsch Bretternhörnli | | 249 | 0.466 | 0.450 | 0.298 10.005 | 305 | 186 | 0.640 | 10.321 | 283 | 0.307 | 14.190 | 85 | 7.01 | 0.01 | 3.05 |
| Rawilpass Lac de Tseuzier Bockialp Klausenpass W Labria Schwarzrüfi Kleintal-Isenthal B Grosstal-Isenthal 1 Isenthal A Kleintal E B Bannalp Betschwanden Haslen Haslen I Mollis Untere Lattreien Glütsch Bretternhörnli | | 249 | 0.489 | 0.439 | 0.280 9.9 | 9.983 | 141 | 0.675 | 10.333 | 309 | 0.281 | 14.129 | <i>L</i> 9 | 6.33 | 0.23 | 2.39 |
| Rawilpass Lac de Tseuzier Bockialp Klausenpass W Labria Schwarzrüfi Kleintal-Isenthal B Grosstal-Isenthal 1 Isenthal A Kleintal E B Bannalp Betschwanden Haslen Haslen 1 Mollis 1 Untere Lattreien Glütsch | | 271 | 0.319 | 0.311 | 0.229 9.9 | 9.962 | 197 | 0.534 | 10.205 | 256 | 0.279 | 14.195 | 70 | 7.56 | 0.02 | 3.45 |
| Rawilpass Lac de Tseuzier Bockialp Klausenpass W Labria Schwarzrüfi Kleintal-Isenthal B Grosstal-Isenthal 1 Isenthal A Kleintal E B Bannalp 1 Betschwanden Haslen Haslen 1 Mollis 1 Untere Lattreien Glütsch Bretternhörnli | | 271 | 0.327 | 0.393 | 0.248 9.9 | 9.983 | 66 | 0.509 | 10.273 | 161 | 0.255 | 14.129 | 41 | 6.46 | 0.04 | 2.35 |
| Lac de Tseuzier Bockialp Klausenpass W Labria Schwarzrüfi Kleintal-Isenthal B Grosstal-Isenthal 1 Isenthal A Kleintal E B Bannalp Bannalp 1 Betschwanden Haslen Haslen 1 Mollis 1 Untere Lattreien Glütsch Bretternhörnli | | 201 | 1.511 | 0.963 | 0.721 10.2 | 10.214 | 162 | 1.338 | 10.974 | 390 | 0.722 | 14.129 | 51 | 4.86 | 0.34 | 1.17 |
| Bockialp Klausenpass W Labria Schwarzrüfi Kleintal-Isenthal B Grosstal-Isenthal I Isenthal A Kleintal E Bannalp Bannalp Haslen Mollis Untere Lattreien Glütsch | | 221 | 0.714 | 0.623 | 0.451 10.097 | 197 | 141 | 0.715 | 10.644 | 88 | 0.231 | 14.129 | 12 | 3.48 | 0.01 | 1.35 |
| Klausenpass W Labria Schwarzrüfi Kleintal-Isenthal B Grosstal-Isenthal 1 Isenthal A Kleintal E B Bannalp Bannalp Haslen Haslen Untere Lattreien Glütsch Bretternhörnli | | 212 | 2.023 | | 0.463 10.023 |)23 | 77 | 1.802 | 11.132 | 244 | 0.315 | 14.206 | 24 | 3.82 | 0.58 | 2.20 |
| Labria Schwarzrüfi Kleintal-Isenthal B Grosstal-Isenthal 1 Isenthal A Kleintal E B Bannalp Bannalp Haslen Haslen Untere Lattreien Glütsch Bretternhörnli | | 211 | 0.516 | 0.507 | 0.334 10.008 | 800 | 297 | 0.704 | 10.255 | 317 | 0.303 | 14.116 | 98 | 5.58 | 0.53 | 1.90 |
| Schwarzrüfi Kleintal-Isenthal B Grosstal-Isenthal 1 Isenthal A Kleintal E B Bannalp Bannalp Haslen Haslen Untere Lattreien Glütsch Bretternhörnli | | 213 | | | 0.424 10.040 |)40 | 45 | 1.590 | 10.974 | 309 | 0.338 | 14.129 | 23 | 4.31 | 69.0 | 5.09 |
| Kleintal-Isenthal B 1 Grosstal-Isenthal 1 Isenthal A Kleintal E B Bannalp 1 Betschwanden Haslen 1 Mollis Untere Lattreien Glütsch Bretternhörnli | | 221 | | 0.917 | _ | 214 | 172 | 1.131 | 10.806 | 483 | 0.683 | 13.870 | 39 | 4.17 | 99.0 | 1.08 |
| B 1 Grosstal-Isenthal 1 Isenthal 1 Isenthal A Kleintal E B Bannalp 1 Betschwanden Haslen 1 Mollis 1 Untere Lattreien Glütsch Bretternhörnli | | 202 | | | | 066.6 | 135 | | 10.605 | 315 | 0.462 | 14.072 | 38 | 5.41 | 0.80 | 1.66 |
| 1 Grosstal-Isenthal 1 Isenthal 1 Isenthal A Kleintal E B Bannalp 1 Betschwanden Haslen 1 Mollis 1 Untere Lattreien Glütsch Bretternhörnli | | 202 | | | | | | | 10.600 | 169 | 0.382 | 14.130 | 13 | 5.18 | 0.43 | 1.91 |
| 1 Isenthal A Kleintal E B Bannalp I Betschwanden Haslen I Mollis Untere Lattreien Glütsch Bretternhörnli | 080 190.720 | 234 | | | | | 7 | | 10.439 | 335 | 0.273 | 14.220 | 44 | 7.45 | 0.82 | 2.17 |
| A Kleintal E B Bannalp 1 Betschwanden Haslen 1 Mollis Untere Lattreien Glütsch | | 234 | | | | 10.018 | | | 10.427 | 162 | 0.278 | 14.158 | 35 | 5.53 | 0.18 | 3.17 |
| A Kleintal E B Bannalp 1 Betschwanden Haslen 1 Mollis Untere Lattreien Glütsch Bretternhörnli | 400 195.650 | 210 | | | | 92(| 123 | _ | 10.682 | 557 | 0.845 | 13.810 | 45 | 5.30 | 0.40 | 1.29 |
| A Kleintal E B Bannalp 1 Betschwanden Haslen 1 Mollis Untere Lattreien Glütsch | | 210 | | | | | 66 | , | 10.773 | 417 | 0.664 | 14.129 | 29 | 4.87 | 0.26 | 1.74 |
| B Bannalp 1 Betschwanden Haslen 1 Mollis Untere Lattreien Glütsch Bretternhörnli | 880 194.670 | 205 | | | | | 274 | | 10.685 | 330 | 0.640 | 14.110 | 55 | 4.96 | 0.48 | 3.56 |
| Bannalp 1 Betschwanden Haslen 1 Mollis Untere Lattreien Glütsch Bretternhörnli | | 205 | | | | | | | 10.773 | 119 | 0.592 | 14.243 | 26 | 5.36 | 0.48 | 1.87 |
| 1 Betschwanden Haslen 1 Mollis 1 Untere Lattreien Glütsch Bretternhörnli | 390 190.810 | 203 | | | | | | , , | 10.579 | 441 | 0.313 | 14.124 | 28 | 5.08 | 69.0 | 4.23 |
| 1 Betschwanden Haslen 1 Mollis Untere Lattreien 1 Glütsch Bretternhörnli | | 203 | | | _ | 187 | | 1.109 | 069.01 | 422 | 0.404 | 14.104 | 99 | 4.80 | 0.56 | 3.04 |
| Haslen 1 Mollis 1 Untere Lattreien 1 Glütsch | 430 200.700 | 256 | | | | 986.6 | | 0.488 | 10.226 | 209 | 0.245 | 14.149 | 28 | 7.33 | 0.00 | 2.51 |
| Haslen 1 Mollis 1 Untere Lattreien 1 Glütsch Bretternhörnli | | 256 | | | | 9.943 | | | 10.190 | 155 | 0.301 | 14.161 | 74 | 5.84 | 0.00 | 4.61 |
| 1 Mollis 1 Untere Lattreien 1 Glütsch Bretternhörnli | | 236 | | | | 9.983 | | | 10.273 | 345 | 0.284 | 14.129 | 75 | 6.93 | 0.11 | 2.78 |
| 1 Untere Lattreien 1 Glütsch Bretternhörnli | 180 217.940 | 216 | | | | 129 | 185 (| | 10.530 | 374 | 0.325 | 14.162 | 63 | 6.26 | 0.02 | 3.77 |
| Untere Lattreien 1 Glütsch Bretternhörnli | | 216 | | | | 000 | 77 | | 10.456 | 116 | 0.796 | 14.418 | 96 | 4.28 | 0.00 | 5.60 |
| 1 Glütsch Bretternhörnli | 780 161.050 | 225 | | 8 | | 000 | 79 | | 10.873 | 172 | 0.485 | 14.101 | 17 | 3.67 | 0.73 | 1.60 |
| Glütsch Bretternhörnli | | 225 | | | | 19 | 66 | 1.185 1 | 10.767 | 221 | 0.440 | 14.176 | 26 | 4.09 | 0.24 | 1.70 |
| Bretternhörnli | 100 159.150 | 234 | 0.713 | | 0.436 10.097 | 161 | 109 | 1.058 1 | 10.580 | 176 | 0.509 | 14.243 | ∞ | 3.68 | 0.22 | 0.81 |
| Bretternhörnli | | 234 | 0.561 | | | 981 | 43 | 1.038 1 | 10.480 | 46 | 0.286 | 14.227 | 9 | 2.04 | 0.13 | 1.17 |
| DICHELINIOLINI | | 226 | | 3 | | 139 | | _ | 10.454 | 117 n | no chlorite | | 4.090.38 | 4.08 | | |
| Barthümeljoch W | | 237 | 0.555 | 0.647 | 0.401 9.9 | 9.983 | 172 | | 10.455 | 405 | 1.044 | 14.129 | 36 | 6.74 | 0.27 | 1.48 |
| Mu-704A Bartümeljoch S 765.770 | 770 213.400 | 237 | 0.880 | 1 | | 170 | 83 (| | 10.640 | 199 | 0.347 | 14.166 | 42 | 4.23 | 0.12 | 2.15 |
| Mu-704B | | 237 | 0.432 | 0.479 | 0.384 10.041 | 141 | 17 | 1.204 | 10.619 | 62 | 0.598 | 14.337 | 21 | 3.83 | 0.64 | 2.04 |

1979) is the result of the overlap of at least two reflections. It is not the consequence of a specific apparatus setting (see e.g. KISCH, 1991), as all samples have been measured with the same apparatus. Scattering effects, such as the fanning of mica layers at their grain boundaries (STERN et al., 1991) are minimized or excluded on the basis of a careful handling of the sample during preparation, e.g. by keeping milling times to less than 30 seconds. The assumption of symmetric peaks is in contradiction to results by Moore and REYNOLDS (1989), which demonstrated increasing tailing of the (001) illite peak with decreasing crystallite size. It is, however, justified in the case of (i) the lack of information about the crystallite size and its evolution with increasing temperature, and (ii) the presence of a clay phase mixture as found in the investigated samples.

(2) X-ray reflections are approximated by Pearson VII functions, which have been shown to provide good fits for both well and poorly crystallized material (STERN et al., 1991).

(3) The d-value of a deconvoluted peak is a resulting parameter, and is not derived from a database X-ray pattern. The applied fitting program optimizes peak positions of pre-selected reflections (d-values), but also peak widths, peak areas/intensities and peak shapes in order to obtain a minimum difference between measured and calculated diffraction pattern (expressed as a reliability factor).

(4) As a consequence of assumption (3), the number of peaks between 4 and 11 °2θ is restricted to a maximum of 3. This is the result of the commonly observable "bull head" (STERN et al., 1991) in samples of diagenetic grade, generated by the presence of two narrow peaks (at about 10 and 14 Å) and a wide peak in-between. The peaks considered are chlorite (with its (001) reflection of 14 Å at about 6.3 °2θ, a "smectitic phase", with variable d-value, and an "illitic-muscovitic phase", with a peak close to the standard (002) muscovite reflection, at around 10 Å (8.8 °2θ). Peak positions were calibrated against the position of the first quartz (100) reflection at 20.9 °2θ.

A large number of additional mineral phases may be expected to show a major reflection within or near the mentioned 2θ-range. Their presence, however, was not confirmed in any sample by reflections of higher order. This particularly applies for mineral phases such as corrensite, paragonite, pyrophyllite, and kaolinite. The presence of most of these phases is in any case unlikely due to bulkrock composition and metamorphic grade of upper diagenetic to lower anchizonal grade. Because of the same argument, the presence of biotite, difficult to recognize by X-ray techniques, can be excluded.

Investigations on fluid inclusions in quartz crystals were made with a Chaixmeca heating and freezing stage, designed to work in the range of – 180 to +600 °C (Poty et al., 1976). Sample preparation and measurement techniques are summarized in MULLIS (1979, 1987). Careful inclusion petrography was needed before inclusions were measured by microthermometry. For this study, only such localities were investigated, where fluid inclusion formation occurred close to the twophase boundary of the methane-bearing waterrich and the water-bearing methane-rich phase. Such conditions were either accomplished within pseudosecondary inclusions of synkinematically grown fibre quartz, or in secondary methanebearing water-rich fluid inclusions of early prismatic quartz, overgrown by skeletal quartz containing primary water-bearing methane-rich inclusions (MULLIS, 1976, 1979, 1987). The homogenization temperature of the earliest methanebearing water-rich fluid inclusions (homogenization of the aqueous phase with the methane bubble) occurs in the laboratory at saturation conditions thought to reflect the approximate formation temperature.

Results

Classic illite "crystallinity" values (determined at the 10 Å complex after KÜBLER et al., 1979) for 71 clay fraction samples vary between 0.30 and 2.02 $\Delta^{\circ}2\theta$ (Fig. 2). The same sample set yields FWHM values for glycolated samples of $0.32-1.12 \Delta^{\circ}2\theta$. The obtained "crystallinity" values illustrate that the metamorphic grade from all sample localities varies from diagenetic to medium-grade anchizone, if applying 0.42 and 0.25 $\Delta^{\circ}2\theta$ as the anchizone boundaries (KÜBLER et al., 1979). A comparison between air-dried values (illite "crystallinity" sensu stricto), and the glycolated values, indicates the presence of swelling components within the measured clay fraction. With beginning of the anchizone (240 \pm 15 °C), there is no longer a visible difference between air-dried and glycolated FWHM values. Within the entire temperature range of 200-270 °C, the difference between airdried and glycolated, however, decreases from nearly $1.0 \Delta^{\circ} 2\theta$ to zero (Fig. 2).

For samples collected at the same locality, a variation in illite "crystallinity" by up to a factor of 2 is observed. This variation in IC values does not show an obvious systematic pattern. In most cases, carbonate-rich samples show smaller IC values than clay-rich samples. There is, however, a small number of samples showing the opposite trend, i.e. higher IC values for carbonate-rich

samples than the clay-rich samples from the same locality. In order to identify the cause for the deviating behaviour, a "dolomite ratio" was defined for the carbonate-rich sample of each locality as the peak intensities of the dolomite (104) main peak (2.89 Å at 31 °20) divided by the sum of the illite/smectite and chlorite peak intensities at 6–10 °20. It was found that samples with a dolomite ratio > 4 systematically display higher IC values than the clay-rich samples. In contrast, carbonate-rich samples with a dolomite ratio < 4 yield smaller illite "crystallinity" values than the clay-rich samples (Fig. 3).

The comparison between fluid inclusion homogenization temperatures (covering a temperature range from 197 to 271 °C) and illite "crystallinity" (Fig. 2) shows a general trend of decreasing peak widths with increasing fluid inclusion temperature. It is evident that the data are characterized by a large scatter in peak width values in the lower half of the temperature range. Here, illite "crystallinity" values may vary between 0.5 and $2.0~\Delta^{\circ}2\theta$ while glycolated peak widths have a reduced vertical scatter of only 0.5 to $1.1~\Delta^{\circ}2\theta$.

By deconvolution, a set of four parameters can be obtained, three of which reveal a trend with increasing temperature. Deconvolution data are given as FWHM values (derived from the deconvoluted α_2 -corrected peaks) and d-values for each separated phase, for this study called "smectitic" and "illitic-muscovitic" phase. For the smectitic phase, values vary considerably between 0.43 and $1.80 \Delta^{\circ}2\theta$ (FWHM) and between 10.205 and 11.182 Å (d-value). In contrast, for the illitic-muscovitic phase the variation is restricted to values between 0.21 and 0.72 $\Delta^{\circ}2\theta$ (FWHM) and between 9.943 and 10.214 Å (d-value). At higher temperatures, all parameters show less scatter and, with exception of the illitic-muscovitic phase. a decrease in d-values (Fig. 4).

A semi-quantitative estimation of the amount of the smectitic phase was achieved by comparing the areas of the deconvoluted smectitic, illitic-muscovitic and chlorite peaks: the smectite content was defined as the area of the smectitic peak divided by the sum of areas of the smectitic, illitic-muscovitic and chlorite peaks. Samples with 35–61% smectitic content tend to show relatively

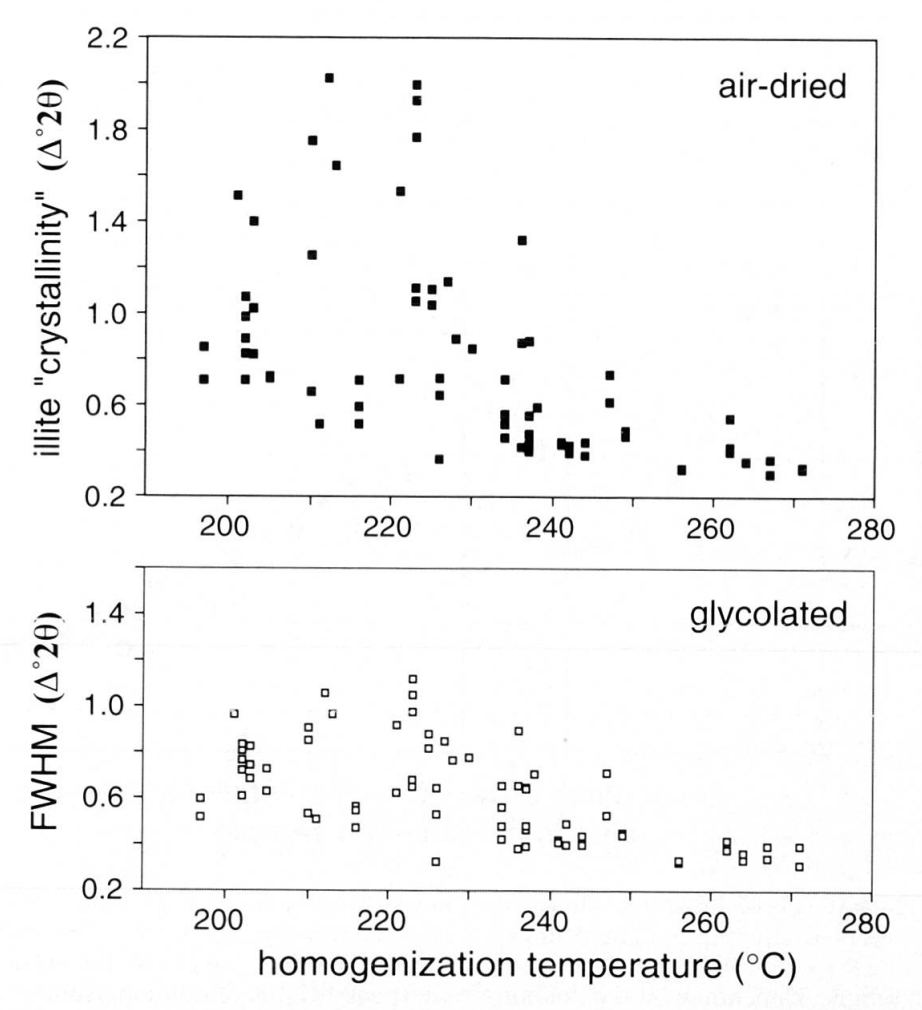


Fig. 2 Measured full width at half maximum (FWHM, unresolved 10 Å complex = illite "crystallinity") for air-dried and glycolated samples versus fluid inclusion homogenization temperature in fibre quartz.

small FWHM values (below 1.2 $\Delta^{\circ}2\theta$, while those with smectitic contents between 62 and 82% show FWHM values of 0.6 to 2.1 $\Delta^{\circ}2\theta$ (Fig. 5).

From the XRF chemical analyses of the $< 2~\mu$ fraction, a statistical evaluation on chemical influences on illite "crystallinity" was carried out. A significant regression factor for correlation with illite "crystallinity" was found for Na. Because both Na and Mg are important elements in smectite phases, the ratio Na₂O/(Na₂O+MgO was chosen as a measure for the presence of smectite in the clay fraction. This ratio shows a distinct correlation with illite "crystallinity" values when plotted against temperature (Fig. 5). Na₂O/(Na₂O + MgO) ratios > 0.08 largely correspond to samples of high

smectite content (62–82%), and these show high illite "crystallinity" values. Na₂O/(Na₂O+MgO) ratios < 0.08 correspond to lower smectite contents (35–61%) and are characterized by lower illite "crystallinity" values. The Na₂O/(Na₂O+MgO) ratio of 0.08 was derived from the applied statistical evaluation and represents a purely empirical value.

The measured K₂O and Na₂O contents of the clay fractions were compared with illite "crystal-linity" values and fluid inclusion homogenization temperatures (Fig. 6). While for Na₂O, only a very faint trend with increasing homogenization temperature is observed, the Na₂O contents in the clay fraction clearly decrease with increasing illite

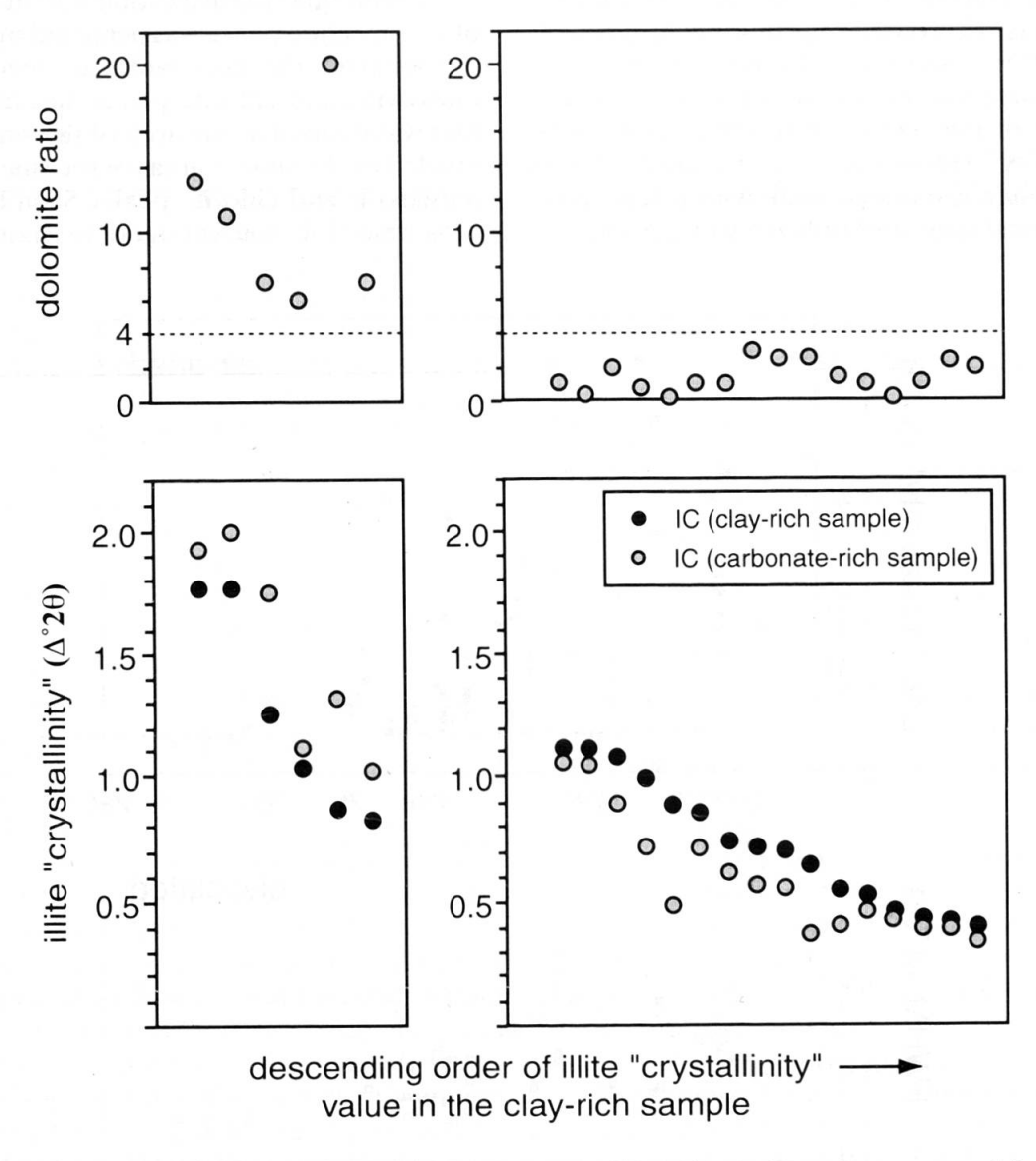


Fig. 3 Diagrams illustrating how illite "crystallinity" depends on the relative carbonate contents and, for carbonate-rich samples, on the relative dolomite contents. Samples are plotted with descending illite "crystallinity" values in the clay-rich sample along the x-axis. Two subgroups are shown, with higher (left) and lower (right) illite "crystallinity" in the carbonate-rich sample. Depending on the dolomite ratio (peak heights of dolomite/sum of clay minerals), carbonate-rich samples with a dolomite ratio > 4 systematically display higher IC values than found for the clay-rich samples. In contrast, carbonate-rich samples with a dolomite ratio < 4 yield smaller IC values than clay-rich samples.

evolution. Trends are even more pronounced for K_2O , which indicates a general increase in the clay fraction with increasing homogenization temperature and a strong increase of K_2O with increasing illite "crystallinity". Similar diagrams for MgO do not show any trends.

Discussion

The assumption that the clay fraction evolves continuously with increasing temperature as an external physical parameter implies that the internal chemical parameters of all investigated samples are constant. Direct comparison of illite "crystallinity" values from different samples as a measure of metamorphic grade is possible only if

the clay fractions of the investigated samples have very similar initial chemical and mineralogical composition and the same chemical environment to evolve towards thermodynamic equilibrium. Under such ideal conditions and provided internal and external parameters reached equilibrium, illite "crystallinity" would represent an absolute measure of the integrated thermal history, similar to vitrinite reflectance (e.g. Sweeney and Burnam, 1991). Any difference in illite "crystallinity" should then correspond to a difference in physical conditions experienced, of which temperature is thought to be the dominant parameter (FREY, 1987).

In reality, illite "crystallinity" is more likely to be a measure of reaction progress than of the thermodynamic equilibrium reached (ESSENE and PEACOR, 1995). The measured "crystallinity"

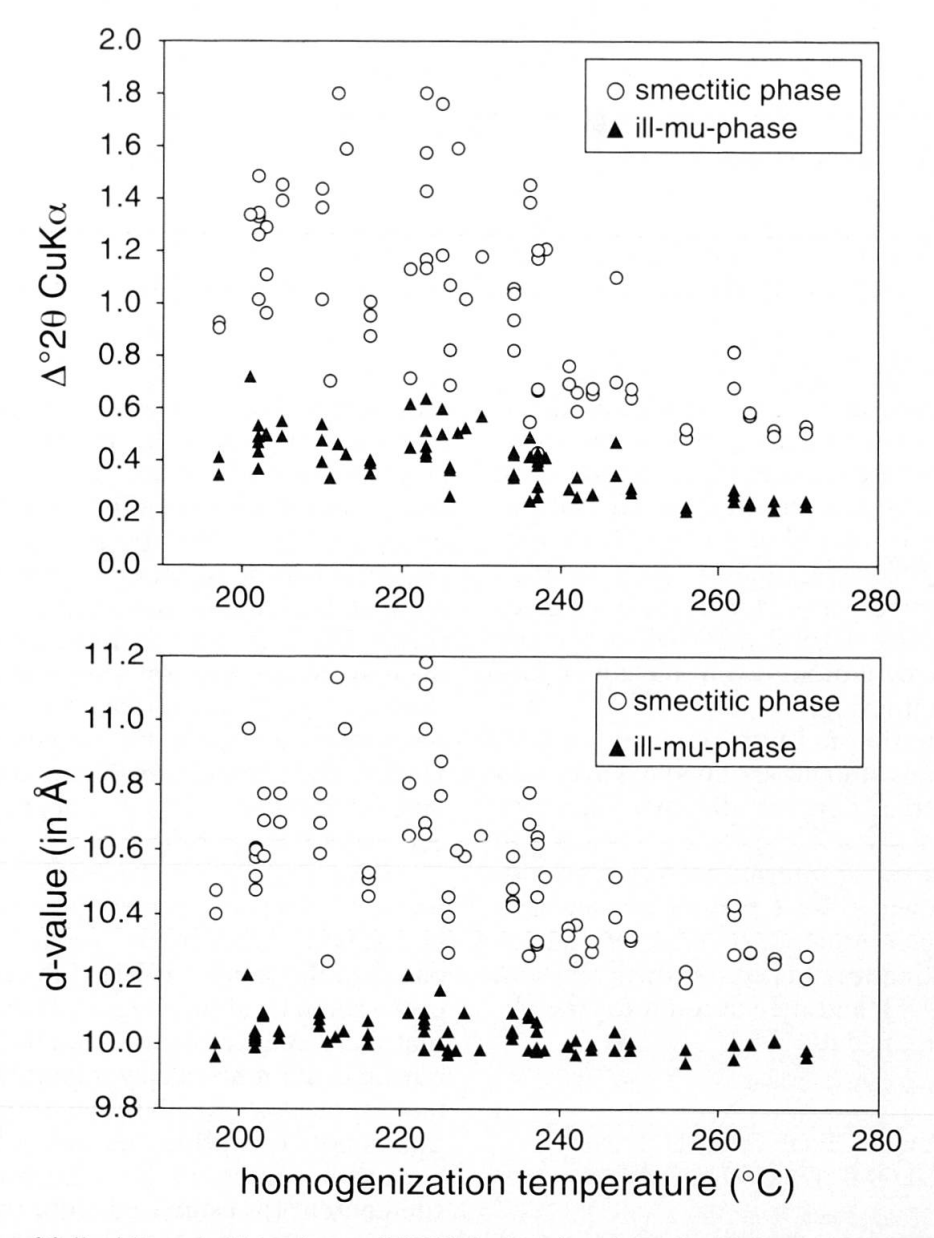


Fig. 4 Evolution of full width at half maximum (FWHM, above) and d-value (below) of the deconvolution fitted smectitic and illitic-muscovitic phase with increasing fluid inclusion homogenization temperature in fibre quartz.

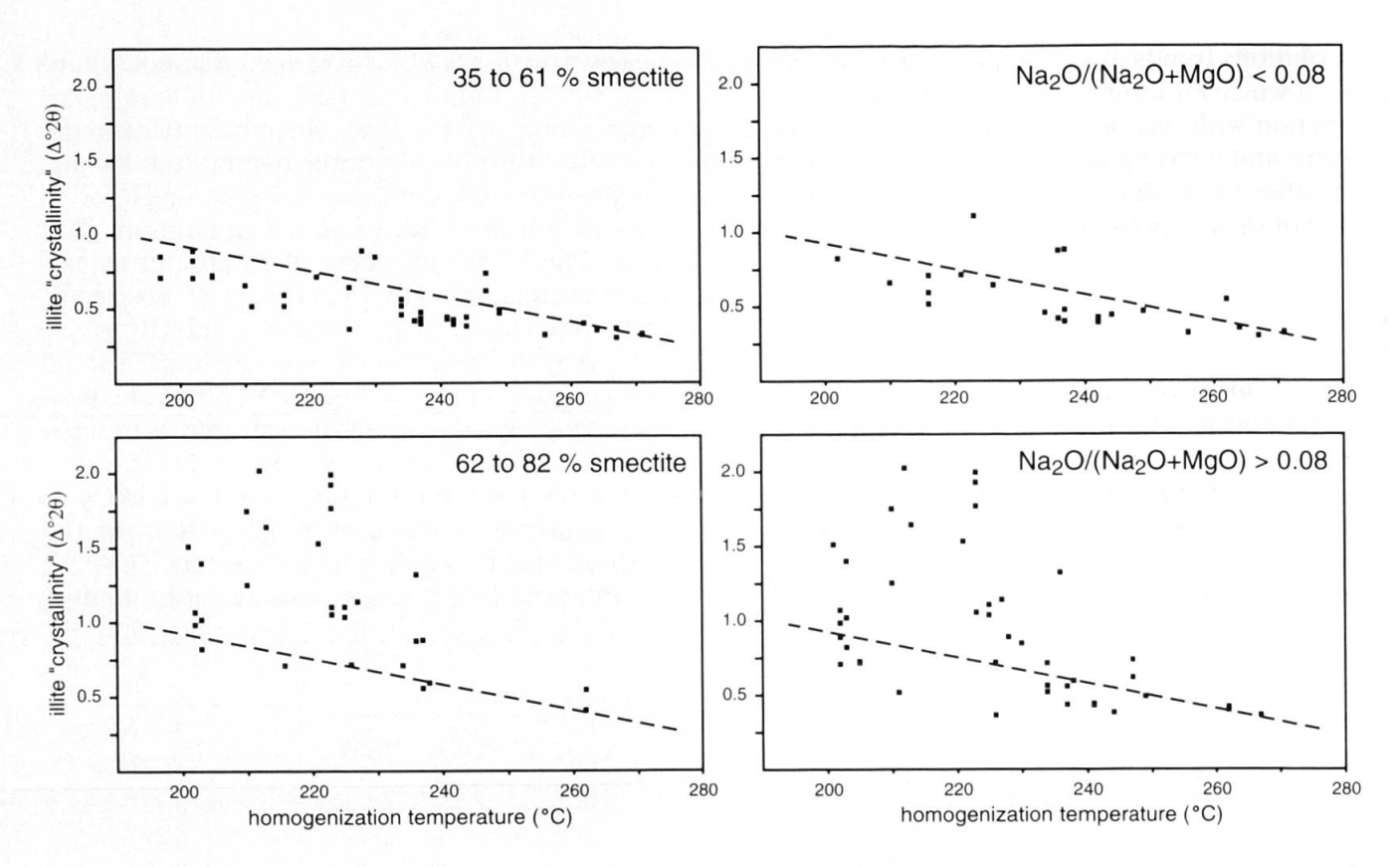


Fig. 5 Relationship between illite "crystallinity" and the smectite content (as defined in the text, diagrams at left) and the clay fraction chemical composition (indicated by the $Na_2O/(Na_2O + MgO)$, as measured on sedimented slides (diagrams at right). For reference only, an arbitrary dashed line is shown; its IC/T_{hom} relationship is the same in all diagrams.

is the result of internal factors, such as composition and crystal size of a detrital clay fraction, and of external factors, such as the supply of nutrients, the structural evolution, as well as physical parameters such as P and T (FREY, 1987; MERRIMAN and PEACOR, 1999). Consequently, illite "crystallinity" is a sensitive parameter of many changes affecting the initial detrital material during the entire thermal evolution, even including late near-surface weathering.

Although the thermal history of the samples investigated in this study is assumed to have been similar, the observed illite "crystallinity" data vary markedly, especially at temperatures below 240 °C. Therefore, a set of internal factors is considered in the following. These factors are shown to have had a distinct influence on illite "crystallinity", i.e. on the kinetics of crystal growth (ESSENE and PEACOR, 1995), and may account for the observed scatter in the data.

THE INFLUENCE OF CALCITE AND DOLOMITE CONTENT

In rocks with little dolomite, illite "crystallinities" are smaller in carbonate-rich rocks than in clay-

rich samples from the same locality (Fig. 3). In the carbonate-rich rocks clay minerals suggest a higher grade of reaction progress as deduced from their lower illite "crystallinity" values. A possible interpretation of the observed pattern is the initial presence of a rather immature, but coarse-grained detrital clay fraction in the carbonate-rich rocks. The structural and chemical evolution of the detrital clay fraction was retarded because the fluid in the carbonate-rich rocks was very probably dominated by Ca, but depleted in K and Na. Under these conditions, the clay fraction remained dominated by detrital grains, and did not evolve with temperature.

Elevated relative contents of dolomite (expressed by the dolomite ratio) correlate with larger FWHM values in carbonate-rich rocks compared to the smaller FWHM in clay-rich samples of the same localities (Fig. 3). It may be suggested that the presence of large quantities of dolomite, but small amounts of clay minerals, may have promoted smectite growth by Mg supply. This suggestion is not convincing, because a comparison between Mg content in the $< 2 \,\mu$ fraction and chlorite content (as estimated from the relative peak area) suggests that samples with much Mg also have high chlorite contents, but not necessarily

high smectite contents (Fig. 5). Therefore, the increased Mg supply will primarily have led to chlorite growth. This assumption can be tested by plotting the relative chlorite peak area (i.e. the chlorite peak area divided by the sum of chlorite, smectitic, and illitic-muscovitic phase areas) against the Na₂O/(Na₂O + MgO) parameter (Fig. 7). From this figure, it is deduced that chlorite is the main carrier of Mg in the clay fraction. A more likely explanation for the relation between dolomite content and larger FWHM is as follows: Dolomite is commonly an important early diagenetic cementation phase, found in many sediments deposited in semi-arid to arid climates (TUCKER and WRIGHT, 1990). Such dolomite cements often precipitate from brines and contain salt-rich fluid inclusions (OVERSTOLZ, 2001), which in turn promote smectite growth. The presence of dolomite would thus be but an indicator, and not a direct cause of increased FWHM values. This explanation is supported by the observation that illite "crystallinity" values are large for both carbonate- and clay-rich samples at those localities,

where the dolomite ratio is large in carbonaterich samples (Fig. 3). It appears that early diagenetic cementation and brines affected carbonaterich rocks as well as the neighbouring shales.

CHEMICAL EVOLUTION OF THE < 2 µ FRACTION

The agreement between the two groups of different smectite contents on one hand, and the different Na₂O/(Na₂O + MgO) ratios on the other (Fig. 5), suggests that most of the smectitic layers present in our samples are Na-bearing. From our data set it cannot be estimated how much Na is incorporated into illite. Paragonite is a common phase reported from clays of anchizonal metamorphic grade (FREY, 1987). All X-ray diffraction patterns, however, were carefully checked for the presence of the paragonite (0010) reflection, but none was found. On the other hand, a comparison between illite "crystallinity" and the K₂O content in the clay fraction (Fig. 6) indicates that anchi-

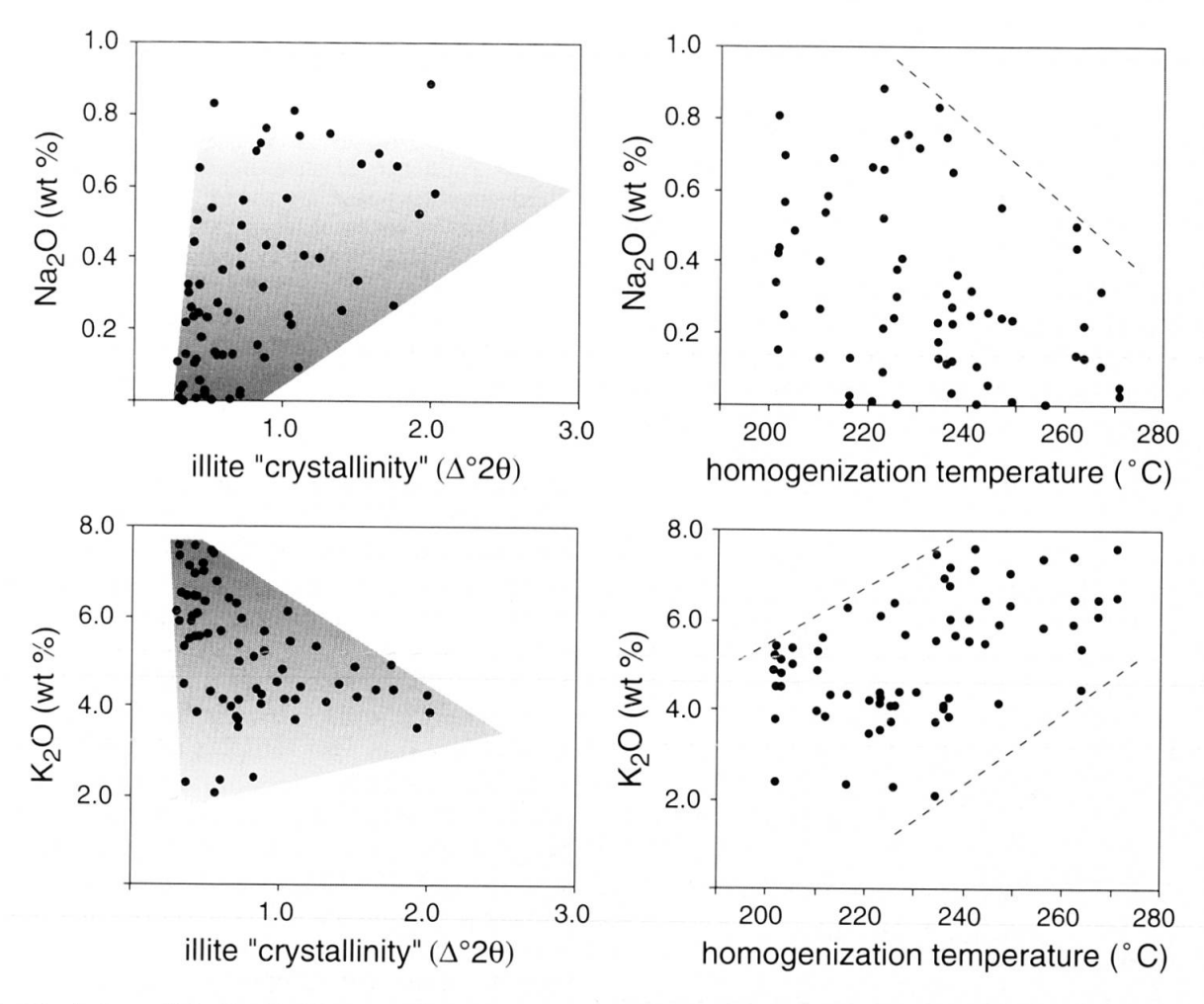


Fig. 6 Evolution of $Na_2O + K_2O$ with increasing illite "crystallinity" (left) and fluid inclusion homogenization temperature (right). At anchizonal conditions, illites become distinctly richer in K, but poorer in Na. Trends are underlined by shaded areas and dashed lines.

zonal illites have K2O contents of up to 8 wt%; this corresponds to an interlayer occupation by K of ~75%. At the same metamorphic grade, the Na₂O content of the illite-smectite complex is reduced to less than 0.8 wt%. We conclude that no paragonite is produced, but the Na content in the illite phase decreases, while the K content increases with increasing temperature. In contrast to a simple reaction between smectite and illite (e.g. Kyser, 2000), the observed quantities of the K_2O take-up and Na₂O loss are not compatible with a simple exchange, as the K₂O gain is one order of magnitude larger than the Na₂O loss. The observed increase of K2O with increasing temperature and the fact that the investigated smectites contain distinctly more Na2O than the illites, requires a source of K outside of the clay fraction during the smectite to illite transition (BORGES et al., 1999; Son et al., 2001). A likely process is the decomposition of K-feldspar with increasing temperature. K-feldspar is not visible in the clay fraction but small amounts of this phase are commonly detected in bulk rock XRD patterns from the shales investigated. In this scenario, illite "crystallinity" would be controlled by an external process.

ILLITE "CRYSTALLINITY" AS A THERMOMETER?

From a simple plot of illite "crystallinity" versus temperature (Fig. 2) it is evident that the variation in the FWHM of the non-deconvoluted X-ray peak complex is markedly influenced by temperature, as well as by the amount of the smectitic phase (Fig. 4). Three samples shown in Fig. 8 illustrate a large scatter of illite "crystallinity" values

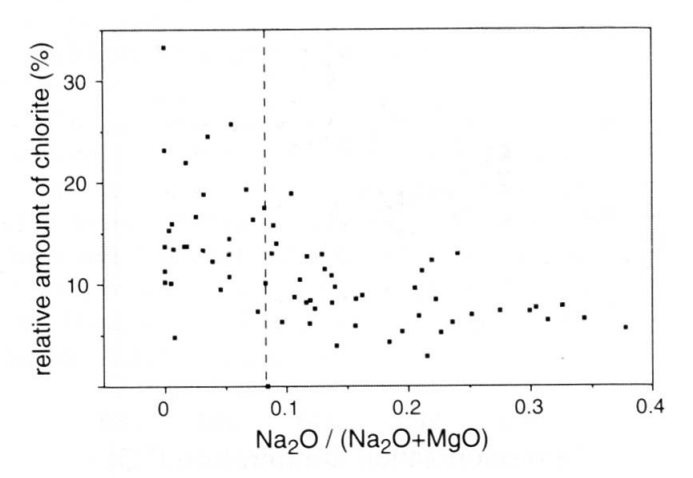


Fig. 7 Relationship between relative chlorite area (see text) and the $Na_2O/(Na_2O + MgO)$ ratio of the clay fraction. The vertical dashed line corresponds to the element ratio of 0.08 (see Fig. 5, diagrams at right).

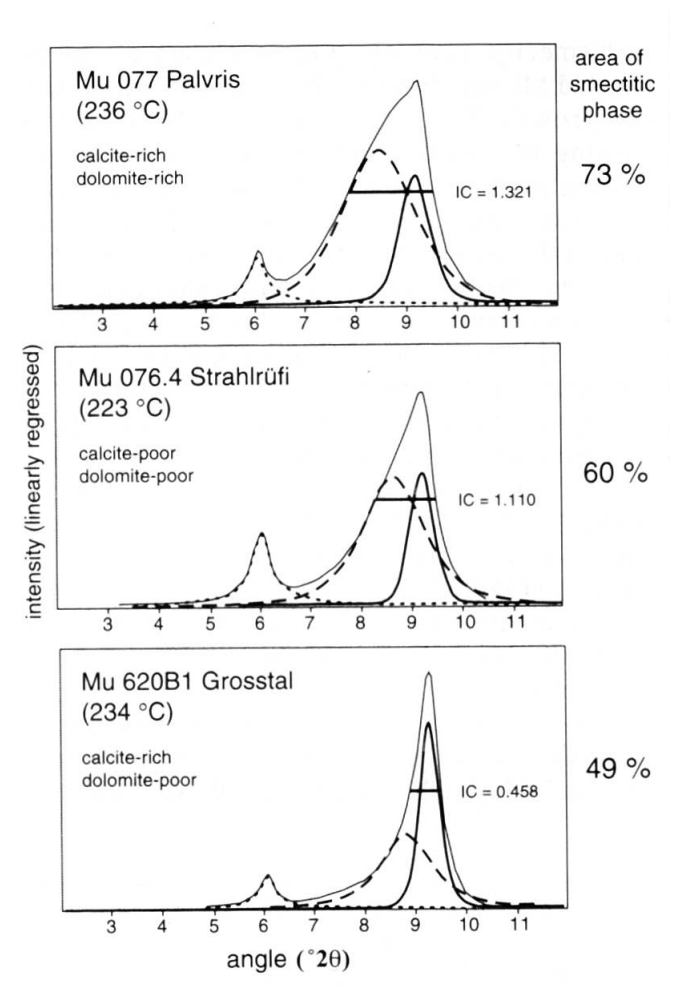


Fig. 8 Influence of smectite content (deconvolution fitted smectitic phase) on the illite "crystallinity" (horizontal bar) at constant temperature. The raw diffractogram is indicated by the enveloping thin line, the deconvoluted phases are an illitic-muscovitic phase (thick line), a smectitic phase (thick dashed line), and chlorite (thick dotted line). Note the variation in carbonate and dolomite content. The indicated IC values are given as $\Delta^{\circ}2\theta$.

at nearly constant maximum temperature conditions (223-236 °C). At the same maximum temperature, the shape of the illite-smectitic peak complex changes from a weakly tailed peak with a position close to pure muscovite to a clearly bimodal distribution, with a saddle between the illite-smectite peak complex and the (001) chlorite peak. The example shown is further complicated by the fact that two samples are carbonate-rich, but dolomite poor, the sample with the largest illite "crystallinity", however, is dolomite-rich. As a consequence, the indicated trend is the result not only of different degrees of smectite formation during peak diagenesis, but also of early diagenesis and fluid composition. Similar observations can be made for samples of equal contents of smectitic phase and homogenization temperatures between 200 and 270 °C. A constant content in smectitic phase, but varying temperature leads

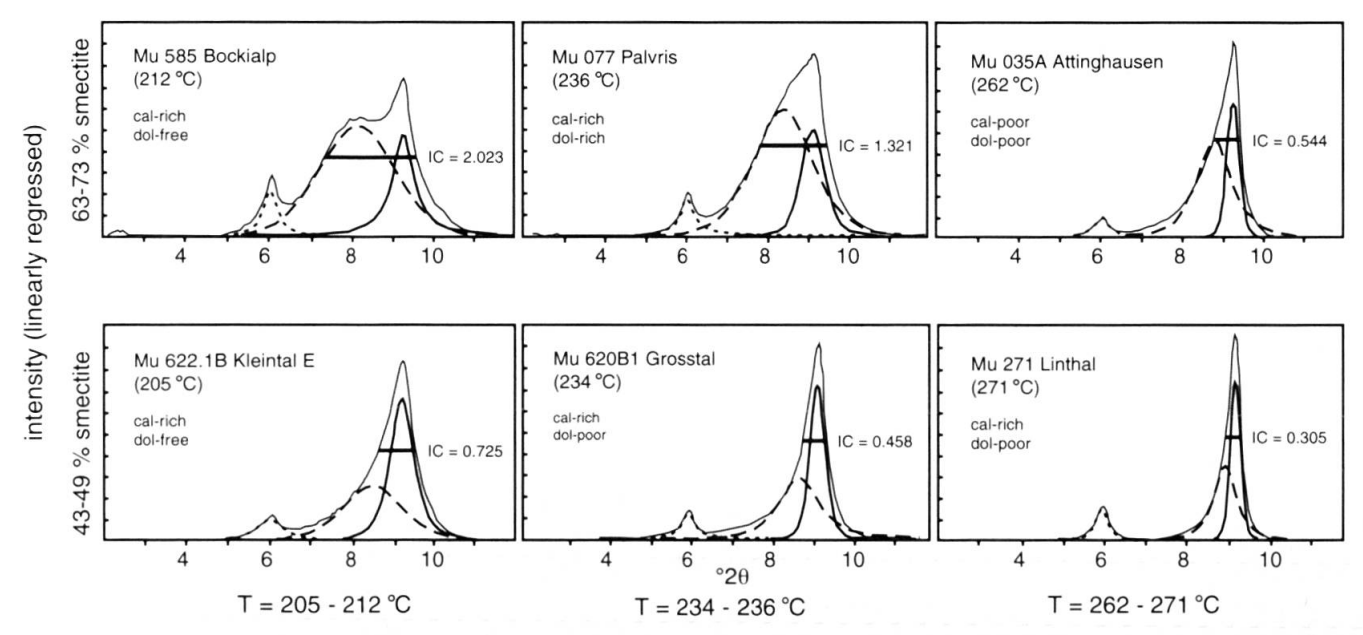


Fig. 9 Development of illite "crystallinity" with increasing fluid inclusion homogenization temperature at different contents of the smectitic phase (taken from deconvolution fitting). For the different stroke patterns, see Fig. 6. Note the different carbonate and dolomite contents at high smectitic phase content, but constant compositional parameters at low smectitic phase content.

to a variation in illite "crystallinity" by a factor 2 (for samples with low smectite contents) to 3 (for samples with high smectite contents) (Fig. 9). While the chosen suite of samples with high smectite contents is strongly variable in dolomite contents, the suite of low smectite samples are all carbonate-rich, but dolomite-poor. These observations raise some doubts about the reliability of the illite "crystallinity" parameter as a thermometer, as previously discussed by MULLIS et al. (1995). Consequently, the relationship between temperature and illite "crystallinity" would also have to include the bulk rock composition and the dolomite content as additional factors. Both of these were shown to be closely linked to the smectite content. A simple relationship between temperature, illite "crystallinity", and smectite content as the major influencing factor (Figs. 8, 9) has been evaluated by multiple linear regression. The correlation is given by:

$$T (^{\circ}C) = 172 - 37*ln (IC) + 0.77*(sm)$$

where IC is the measured illite "crystallinity" in $\Delta^{\circ}2\theta$, and (sm) is the percentage of smectitic phase as obtained from deconvolution fitting with symmetric Pearson VII functions. The 1σ errors of the fitted parameters are: 172 ± 17 (=10% relative error), 37 ± 5 (13%), and 0.77 ± 0.27 (35%), and the reliablity of the statistical fitting is expressed by a regression factor r^2 of 0.51 and a reduced $\chi^2 = 15$ (n = 71). The errors illustrate that the content of smectitic phase is the least well constrained pa-

rameter in the mentioned relationship. The relation also underlines that illite "crystallinity" as an indicator of incipient metamorphism is a semi-quantitative measure at best. The same is true for "crystallinity" parameters derived from deconvolution, i.e. a "smectitic phase crystallinity" or "illitic-muscovitic phase crystallinity" (Fig 4).

TEMPERATURE OF THE DIAGENESIS-ANCHIZONE BOUNDARY

The diagenesis-anchizone boundary was defined by KÜBLER (1967) at an illite "crystallinity" value of 0.42 Δ °2 θ . In our data set, diagenetic IC values are found up to (fluid inclusion derived) temperatures of 260 °C, while the first anchizonal value occurs at T = 225 °C (Fig. 10). The scatter in illite "crystallinity" is large below and strongly reduced above 240 °C. The diagenesis-anchizone boundary is interpreted to be around 240 \pm 15 °C, i.e. at much higher temperatures than previously assumed (e.g. FREY, 1986). Based on the present data, a typical sample at 240 °C contains a calculated content of 40% of smectitic phase with a FWHM of $0.95 \,\Delta^{\circ}2\theta$ and a peak position at $10.5 \,\text{Å}$ (Fig. 4). The illitic-muscovitic peak has a FWHM of $0.35 \Delta^{\circ} 2\theta$ and a d-value of 10.0 Å.

The obtained diagenesis-anchizone boundary is consistent with estimates based on other observations such as vitrinite reflectance (e.g. FERREI-RO-MÄHLMANN, 1996) and mineral parageneses (e.g. RAHN et al., 1994). The presence of a peak

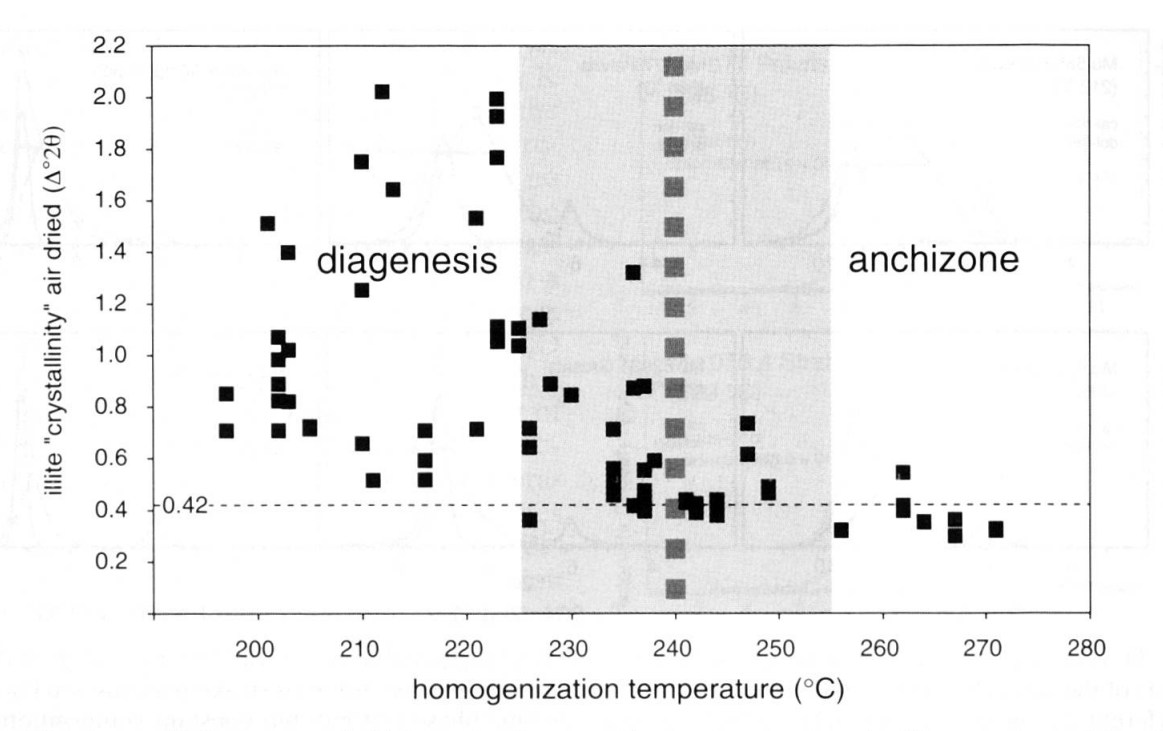


Fig. 10 Illite "crystallinity" versus fluid inclusion homogenization temperature in fibre quartz and the derived anchizone temperature boundary at Δ °20 = 0.42 (KÜBLER et al. 1979). The uncertainty of the diagenesis-anchizone boundary temperature (± 15 °C) is indicated by the grey area.

corresponding to 40% of the smectitic phase cannot be translated directly to 40% of a swelling phase, which would be in contradiction to the initial definition of the anchizone, as a metamorphic level without any swelling component (KÜBLER, 1967). The comparison between air-dried and glycolated FWHM values of the unresolved illitesmectite complex at 10Å (Fig. 2) indicates that, with beginning of the anchizone at 240 °C, glycolation does not significantly change the FWHM values. The major reason for the calculated presence of 40% smectitic phase is probably the assumption of solely symmetric reflections used for deconvolution. Moore and REYNOLDS (1989) showed that the asymmetry of the (001) illite peak is a function of crystallite size and hence of metamorphic grade. We submit that part of the calculated smectitic content may be an artefact.

The temperature of 240 °C obtained for the diagenesis-anchizone boundary should be tested in other terranes in order to ascertain whether it is generally applicable or typical only of a fast evolution as in the European Alps, with moderate pressure conditions, and a time span of approximately 30 million years between burial (defined e.g. by the age of the Taveyannaz event, RUFFINI et al., 1997) and final exhumation of the samples. Furthermore, the influence of the lithology on illite "crystallinity" (e.g. in BREITSCHMID, 1982) has to be evaluated in more detail.

Conclusions

The investigated samples from the external part of the Central Alps cover a range of maximum temperatures between 200 and 270 °C (based on fluid inclusion data). Illite "crystallinity" measurements and mathematical deconvolution procedures defining the FWHM and d-values of a smectitic and an illitic-muscovitic phase justify the following confusions:

- (a) Bulk rock composition (from shale to marly limestone) has a distinct influence on illite "crystallinity" values, by lowering peak widths by a factor of up to 2 in carbonate-rich samples (Fig. 3).
- (b) Dolomite-rich samples with minor clay content can have very high illite "crystallinity" values. Rather than acting as a source of Mg for smectite formation, dolomite indicates early diagenetic high saline fluids, which lead to the formation of Na-bearing smectite in both carbonate-and clay-rich samples.
- (c) The amount of smectitic phase (determined by deconvolution) shows a close relationship with the composition of the $< 2 \mu$ fraction, notably its Na₂O/(Na₂O + MgO) ratio, indicating that smectite has high Na contents.
- (d) A correlation between the classic illite "crystallinity" parameter, the content of the smectitic phase, and temperature was used to test how reliable a thermometer illite "crystallinity" is. The accuracy of the derived thermometer turns out to

be restricted due to bulk rock variation and its influence on the smectite-illite transition.

(e) For the investigated external parts of the Central Alps, the comparison between illite "crystallinity" and fluid inclusion temperatures indicates that the boundary diagenesis-anchizone is located at a temperature of 240 ± 15 °C. At diagenetic conditions, illite "crystallinity" cannot be used as a temperature indicator, except for samples of well-defined lithologies of constant composition. Above 240 °C, across different lithologies, illite "crystallinity" values show considerably less scatter and serves as an approximate temperature indicator. The distinct increase in K₂O, parallel to a much smaller decrease in Na₂O, requires a K source outside the clay fraction.

Acknowledgements

Martin Frey and Bernard Kübler were the spiritual fathers for the present contribution. Thankfully we remember their stimulating and critical discussions in our future work. We like to thank M. Engi and L. Warr for their constructive reviews. Helpful contributions to data processing were provided by M. Sun and H. Wang. T. Heijboer helped with figure drawing. Financial support for this study was given by grants of the Swiss National Science Foundation to the first two authors (21-27.555.89 and 21-33868.92), and by travel grants to the authors by the University of Basel, the Freiwillige akademische Gesellschaft, Basel, and the Albert-Ludwigs-Universität Freiburg (to M. Rahn).

References

BAULUZ, B., PEACOR, D.R. and GONZALEZ-LOPEZ, J.M. (2000): Transmission electron microscopy study of illitization in pelites from the Iberian Range, Spain; layer-by-layer replacement? Clays and Clay Miner. 48, 374–384

BORGES, J.B., MACK, D.M., HANAN, M.A. and TOTTEN, M.W. (1999): Clay-mineral diagenesis in the Louisiana Gulf Coast, how much K is needed for the smectite-illite transition. Abstracts with Programs. Geol.

Soc. America 31, p. 160.

Breitschmid, A. (1982): Diagenese und schwache Metamorphose in den sedimentären Abfolgen der Zentralschweizer Alpen (Vierwaldstätter See, Urirotstock). Eclogae geol. Helv. 75, 331–380. ERDELBROCK, K. (1994): Diagenese und schwache

Metamorphose im Helvetikum der Ostschweiz (Inkohlung und Illit-"Kristallinität"). Unpubl. Ph.D. thesis, Univ. Aachen, 220 pp.

ESSENE, E.J. and PEACOR, D.R. (1995): Clay mineral thermometry – a critical perspective. Clays and Clay

Miner. 43, 540-553.

FERREIRO-MÄHLMANN, R. (1994): Zur Bestimmung von Diagenesehöhe und beginnender Metamorphose – Temperaturgeschichte und Tektogenese des Austroalpins und Südpenninikums in Vorarlberg und Mittelbünden. Frankfurter geowissenschaftliche Arbeiten, Serie C, 14, 498 pp.

FERREIRO-MÄHLMANN, R. (1995): Das Diagenese-Metamorphose-Muster von Vitrinitreflexion und Illit-"Kristallinität" in Mittelbünden und im Oberhalbstein; Teil 1, Bezüge zur Stockwerktektonik.

Schweiz. Mineral. Petrogr. Mitt. 75, 85–122. FERREIRO-MÄHLMANN, R. (1996): Das Diagenese-Metamorphose-Muster von Vitrinitreflexion und Illit-"Kristallinität" in Mittelbünden und im Oberhalbstein; 2, Korrelation kohlenpetrographischer und mineralogischer Parameter. Schweiz. Mineral. Petrogr. Mitt. 76, 23-46.

FREY, M. (1986): Very low-grade metamorphism of the Alps – an introduction. Schweiz. Mineral. Petrogr.

Mitt. 66, 13-27

FREY, M. (1987): Very low-grade metamorphism of clastic sedimentary rocks. In: FREY, M. (ed.): Low temperature metamorphism. Blackie & Son, Glasgow. p.

Frey, M., Teichmüller, M., Teichmüller, R., Mullis, J., KUENZI, B., BREITSCHMID, A., GRUNER, U. and SCHWIZER, B. (1980): Very low-grade metamorphism in external parts of the Central Alps; illite crystallinity, coal rank and fluid inclusion data. Eclogae geol. Helv. 73, 173-203.

JABOYEDOFF, M., BUSSY, F., KÜBLER, B. and THÉLIN, P. (2001): Illite "crystallinity" revisited. Clays and Clay

Miner. 49, 156-167.

KISCH, H. (1991): Illite crystallinity: recommendations on sample preparation, X-ray diffraction settings, and interlaboratory samples. J. Metamorphic Geol.

KÜBLER, B. (1967): La cristallinité de l'illite et les tones tout à fait supérieures du métamorphisme. In: Étages tectoniques, Colloque de Neuchâtel 1966, À la

Baconnière, Neuchâtel, Suisse, 105–121. KÜBLER, B., PITTION, J.-L., HEROUX, Y., CHAROLLAIS, J. et WEIDMANN, M. (1979): Sur le pouvoir réflecteur de la vitrinite dans quelques roches du Jura, de la Molasse et des Nappes préalpines, helvétiques et penniniques. Eclogae geol. Helv. 72, 347–373.

KYSER, K. (2000): Fluids and basin evolution. Short course Handbook 28. Mineral. Assoc. Canada, Otta-

wa, 262 pp.

LANSON, B. and CHAMPION, D. (1991): The I/S-to-illite reaction in the late stage diagenesis. Am. J. Sci. 291, 473-506.

Lanson, B. and Besson, G. (1992): Characterization of the end of smectite-to-illite transformation; decomposition of X-ray patterns. Clays and Clay Miner. 40, 40-52

LANSON, B. and VELDE, B. (1992): Decomposition of Xray diffraction patterns; a convenient way to describe complex I/S diagenetic evolution. Clays and Clay Miner. 40, 629–643.

MERRIMAN, R.J. and PEACOR, D.R. (1999): Very lowgrade metapelites: mineralogy, microfabrics and measuring reaction progress. In: FREY, M. and ROB-INSON, D. (eds): Low-Grade Metamorphism, Blackwell Science, Oxford, 10-60.

MOORE, D.M. and REYNOLDS, R.C. (1989): X-ray diffraction and identification of clay minerals. Oxford Uni-

versity Press, Oxford.

MULLIS, J. (1976): Das Wachstumsmilieu der Quarz-kristalle im Val d'Illiez (Wallis, Schweiz). Schweiz. Mineral. Petrogr. Mitt. 52, 219-268.

MULLIS, J. (1979): The system methane-water as a geologic thermometer and barometer from the external part of the Central Alps. Bull. Minéral. 102, 526–536.

MULLIS, J. (1987): Fluid inclusion studies during very low-grade metamorphism. In: FREY, M. (ed.): Low temperature metamorphism. Blackie & Son, Glasgow. p. 162-199.

MULLIS, J. (1997): The application of fluid inclusions to fluid geochemistry and geothermobarometry in diagenetic and low-grade metamorphic rocks in the exernal parts of the Central Alps. XIV ECROFI European current Research on Fluid Inclusions, Nancy, France, July 1–4, 1997. M.C. Boiron and J. Pironon (eds): Abstract Volume, 224–225.

MULLIS, J., DUBESSY, J., POTY, B. and O'NEIL, J. (1994): Fluid regimes during late stages of a continental collision: Physical, chemical and stable isotope measurements of fluid inclusions in fissure quartz from a geotraverse through the Central Alps, Switzerland. Geochim. Cosmochim. Acta 58, 2239-2267.

MULLIS, J., RAHN, M., DE CAPITANI, C., STERN, W.B. and FREY, M. (1995): How good is illite "crystallinity" as a geothermometer? Abstract supplement 1, Terra

nova 7, 128-129.

OVERSTOLZ, M. (2001): Diagenesis of Triassic Bunter Gas reservoirs in field "A" and surrounding fields, West Netherlands Basin. Unpubl. diploma thesis, Univ. of Basel, 50 pp.

POTY, B., LEROY, J. and JACHIMOWICZ, L. (1976): Un nouvel appareil pour la mesure des températures sous le microscope: l'installation de microthermométrie Chaixmeca. Bull. Minéral. 99, 182–186.

RAHN, M., MULLIS, J., ERDELBROCK, K. and FREY, M. (1994): Very low-grade metamorphism of the Taveyanne greywacke, Glarus Alps, Switzerland. J. Metamorphic Geol. 12, 625-641.

RAHN, M.K., MULLIS, J., ERDELBROCK, K. and FREY, M. (1995): Alpine metamorphism in the North Helvetic flysch of the Glarus Alps, Switzerland. Eclogae geol.

Helv. 88, 157–178.

ROBINSON, D. and SANTANA DE ZAMORA, A. (1999): The smectite to chlorite transition in the Chipilapa geothermal system, El Salvador. Am. Mineralogist 84, 607-619.

Ruffini, R., Polino, R., Calleghari, E., Hunziker, J.C. and Pfeiffer, H.-R. (1997): Volcanic clast-rich turbidites of the Taveyanne sandstones from the Thônes syncline (Savoie, France): records for a Tertiary postcollisional volcanism. Schweiz. Mineral. Petrogr. Mitt. 77, 161-174.

Son, B.K., Yoshimura, T. and Fukasawa, H. (2001): Diagenesis of dioctahedral and trioctahedral smectites from alternating beds in Miocene to Pleistocene rocks of the Niigata Basin, Japan. Clays and

Clay Miner. 49, 333-346.

Stern, W.B., Mullis, J., Rahn, M. and Frey, M. (1991): Deconvolution of the first "illite" basal reflection. Schweiz. Mineral. Petrogr. Mitt. 71, 453–462.

SWEENEY, J.J. and BURNAM, A.K. (1991): Evaluation of a simple model of vitrinite reflectance based on chemical kinetics. Am. Assoc. Petrol. Geol. Bull. 74, 1559-1570.

TUCKER, M.E. and WRIGHT, V.P. (1990): Carbonate Sedi-

mentology. Blackwell Sci. Publ., Oxford.

WANG, H., FREY, M. and STERN, W.B. (1996): Diagenesis and metamorphism of clay minerals in the Helvetic Alps of eastern Switzerland. Clays and Clay Miner. 44, 96–112.

Manuscript received February 7, 2002; revision accepted June 11, 2002 Editorial handling: M. Engi